Journal of Marine Science and Technology

Volume 24 | Issue 6 Article 6

IMPACT OF CLIMATE CHANGE ON SHIHMEN RESERVOIR WATER SUPPLY

Tai-Yi Chu
Department of Harbor and River Engineering, National Taiwan Ocean University, Keelung, Taiwan, R.O.C.

Jyun-Long Lee
Department of Harbor and River Engineering, National Taiwan Ocean University, Keelung, Taiwan, R.O.C.

Wen-Cheng Huang
Department of Harbor and River Engineering, National Taiwan Ocean University, Keelung, Taiwan, R.O.C.,
b0137@mail.ntou.edu.tw

IMPACT OF CLIMATE CHANGE ON SHIHMEN RESERVOIR WATER SUPPLY

Acknowledgements

The authors express appreciation to the National Taiwan University Global Change Center for providing relevant downscaled GCMs. This study was sponsored by a project of the Council of Agriculture under the Executive Yuan of Taiwan (102AS-8.2.4-IE-b2 and 103AS-8.2.6-IE-b1).

Journal of Marine Science and Technology, Vol. 24, No. 6, pp. 1093-1104 (2016)
DOI: 10.6119/JMST-016-1004-1

IMPACT OF CLIMATE CHANGE ON SHIHMEN RESERVOIR WATER SUPPLY

Tai-Yi Chu, Jyun-Long Lee, and Wen-Cheng Huang

Key words: climate change, Shihmen reservoir, tank model, risk.

ABSTRACT

This study evaluated the impact of climate change on the water supply of the Shihmen reservoir in northern Taiwan. Five downscaled general circulation models that represent the daily meteorological data of 2046-2065 were adopted. The future inflow of the Shihmen reservoir was estimated using the tank model. Subsequently, the water supply risk under the given demand and operating conditions was simulated and assessed.

Compared with 2004-2011, the average annual precipitation of the Shihmen watershed in 2046-2065 is lower, particularly during the wet season (May-October). Therefore, the risk to the water supply will increase in the first cropping season (from March to June) in the future. To reduce the risk of water shortage caused by public demand, irrigation fallowing during the cropping season is necessary.

I. INTRODUCTION

Climate change has been a public concern in recent years. As the most authoritative institution for climate change, the Intergovernmental Panel on Climate Change (IPCC) has published many assessment reports since 1990, and has continued to highlight the impact of climate change on human and natural systems. The IPCC noted in its fourth assessment report (AR4) that the observed increase in global average temperatures since the mid-20th century is very probably a result of the observed increase in anthropogenic greenhouse gas (GHG) concentrations (IPCC, 2007). In its fifth assessment report (AR5), the IPCC repeated this assertion and emphasized that anthropogenic GHGs are extremely likely to have been the dominant cause of the observed warming. Projected changes in the climate system are mentioned in the AR5: The surface temperature and global mean sea level are projected to rise over the twenty-first century; meanwhile, it is very likely that heat waves will occur more often and for longer durations, and that more intense and frequent rainstorms will occur in many regions (IPCC, 2014).

Taiwan is a small island on the west Pacific, and it is considerably affected by climate change (Asia Development Bank, 2009). Wu et al. (2013) analyzed meteorological records of 1911-2009 and concluded that temperature increased 0.14°C per decade on average, but during 1980-2009, it increased at the higher rate of 0.29°C per decade. For precipitation, a linear trend was nonsignificant; however, the number of rainy days consistently decreased.

Many local studies have addressed the future impacts of climate change on Taiwan (Yu, 2006; Liu et al., 2008; Lin et al., 2009; Hsu et al., 2011; Huang et al., 2012; Huang et al., 2014). The literature suggests that in general, temperatures will increase, and the temporal distribution of precipitation will become more uneven. Moreover, some studies have emphasized that the frequency of rainless days will increase (Lin et al., 2009; Huang et al., 2012; Huang et al., 2014). These changes present challenges for water resource management in Taiwan.

The Shihmen reservoir is a major water supply resource in northern Taiwan (Fig. 1). The reservoir supplies irrigation and public water demands in Taoyuan County and parts of New Taipei City. The watershed area of the Shihmen reservoir is 763.4 km^2. Its effective storage is approximately 2.1×10^8 m^3, and the average annual supply for public use is 4.6×10^8 m^3 (Northern Region Water Resources Office, 2014). Moreover, the Taoyuan Aerotropolis project has been approved and is ready to commence. Thus, it is clear that pressure on the Shihmen reservoir will increase.

In previous studies, we have discussed the impact of climate change on the irrigation water requirements for the areas of the Shihmen Irrigation Association (SIA) and Taoyuan Irrigation Association (TIA), the two irrigation areas that the Shihmen reservoir supplies (Huang et al., 2013; Lee and Huang, 2014). Climate change scenarios suggest that both rainfall and temperature will increase. For the SIA, future irrigation water requirements will decrease significantly in both cropping seasons (9.1% for the first and 18.4% for the second) because of increases in effective rainfall. By contrast, an insignificant change (< 2.5%) is projected for the TIA because the increase in effective rainfall will be neutralized increased crop water requirements.

After previously assessing the impact of climate change on the demand of the Shihmen reservoir, in this study, we focused on assessing of the impact of climate change on both the reservoir inflow and the risk to the water supply of the Shihmen reservoir.

Paper submitted 02/03/16; revised 07/13/16; accepted 10/04/16. Author for correspondence: Wen-Cheng Huang (e-mail: b0137@mail.ntou.edu.tw).
Department of Harbor and River Engineering, National Taiwan Ocean University, Keelung, Taiwan, R.O.C.

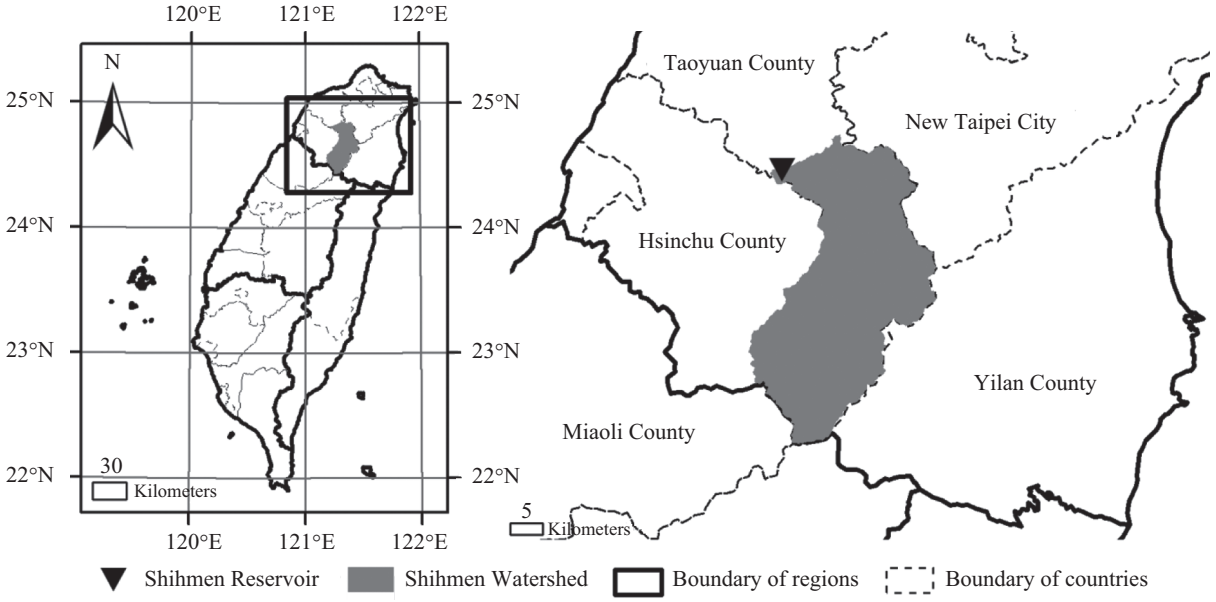

Fig. 1. Location of the Shihmen reservoir and watershed.

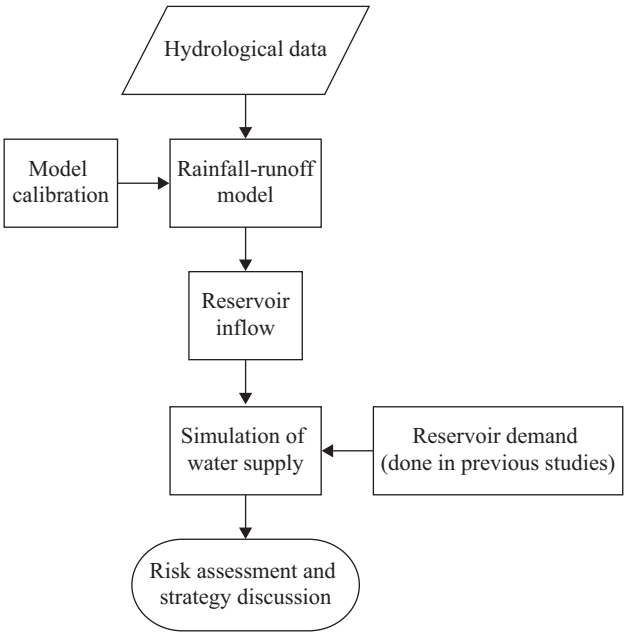

Fig. 2. Flowchart of this study.

II. MATERIALS AND METHODS

Future inflow of reservoirs under climate change should be evaluated. Therefore, daily hydrological data such as precipitation and temperature, both observed and projected, are required. An applicable rainfall-runoff model is also necessary. On the basis of its demand and regulations, the water supply system of the Shihmen reservoir was simulated to assess future water supply risk.

In this study, the present and future meteorological situations were assessed using the periods of 2004-2011 and 2046-2065, respectively. The study flowchart is depicted in Fig. 2.

1. Projected Precipitation and Temperature

General circulation models (GCMs) are the most advanced tools available for simulating the response of the global climate system to increasing GHG concentrations. We used the AR4 GCMs employed by previous studies (Huang et al., 2013; Lee and Huang, 2014) as input instead of the AR5 GCMs for consistency.

The projected precipitation and temperature under climate change for 2046-2065 were derived from five GCMs: CGCm3 from the Canadian Center for Climate Modeling and Analysis (CCCma), Cm3 from the Centre National de Recherches Meteorologiques (CNRM), Mk3.0 from Australia's Commonwealth Scientific and Industrial Research Organization (CSIRO), Cm2.0 from the Geophysical Fluid Dynamics Laboratory (GFDL) and FGOALS-g1.0 from the State Key Laboratory of Numerical Modeling for Atmospheric Sciences and Geophysical Fluid Dynamics (LASG), which are based on SRES A1B scenarios. The A1B scenario describes a future world of very rapid economic growth, a global population that peaks mid-century and declines thereafter, and the rapid introduction of new and more efficient technologies. Moreover, the A1B scenario is distinguished by its technological emphasis: a balance across fossil fuels and other energy sources (IPCC, 2007).

Because of the coarse resolution of GCM projections, the GCM scenario-run outputs required statistical downscaling at local climate stations. All data were downscaled by the Global Change Research Center of National Taiwan University. Briefly, the process of downscaling was performed in three stages (Lin et al., 2010). First, the GCM outputs near Taiwan were adjusted with respect to the NCEP reanalysis data (Kalnay et al., 1996), during the training period by linking the normalized

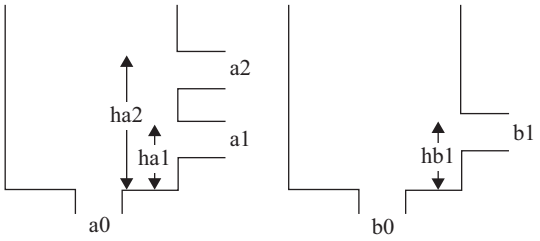

Fig. 3. 2-layer Tank model.

probability distribution functions of the mean climate parameters. Second, a transfer function (i.e., a multiple-variant linear regression) was established to link NCEP reanalysis variants with local climatic observations from the training period. Third, the projected temperature and precipitation data collected at each station during the verification period were adjusted according to the local observation data by repeating the procedure used in the first stage. The established linkage was then extended to adjust outputs for the projected years. For further details of the downscaling technique, please refer to Lin et al. (2009) and Lin et al. (2010).

2. Rainfall-Runoff Model

1) Tank Model

To assess the inflow under climate change, the tank model, a conceptual and deterministic rainfall-runoff model, was adopted in this study. This model comprises several tanks and considers the storage effect of the watershed. Therefore, the runoff response of the different layers of the watershed—surface runoff, subsurface runoff, and base flow—was simulated appropriately (Sugawara, 1985). The advantages of the tank model include a simple structure, easy calculations, and reasonable function (Yokoo and Kazama, 2012). However, the model used in this study differs from the classic four-layer model that Sugawara proposed. A two -layer tank model mitigates the storage effect and is more applicable to the Shihmen reservoir watershed (Fig. 3) because the average slope of the Shihmen watershed is higher than that of watersheds in Japan.

In the conceptual model, the top of the two-layer tank model represents the mechanism of surface runoff in a watershed. A watershed becomes saturated when precipitation fills the top tank to a height of ha1. When the water level in the top tank surpasses ha1, excess precipitation exits the tank through orifice a1. This process is the major component of surface runoff. In a rage storm, the water level in the top tank is higher than ha2, and the outflow through orifice a2 represents the runoff in this case. Orifice a0 simulates the percolation process in a watershed, in which the water is transported into the ground. The bottom of the two-layer tank model represents the interflow and groundwater mechanisms and is opposite to the top layer. Parameter hb1 is a threshold similar to ha1. The discharge through orifice b1 represents the outflow of interflow and groundwater, and the discharge through orifice b0 represents deep infiltration in the watershed.

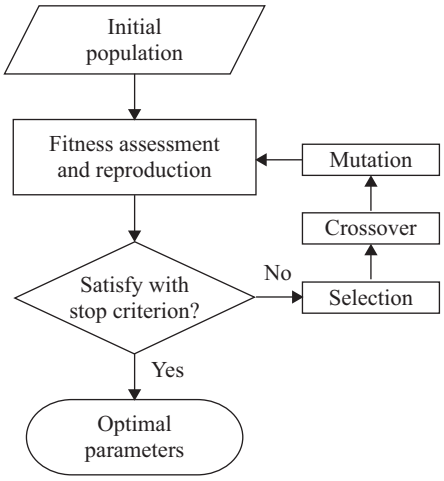

Fig. 4. Flowchart of the Genetic Algorithm.

Only a fraction of the total precipitation reaches the tank because of evapotranspiration, which is one of the crucial influences on watershed runoff. The Penman-Monteith (PM) equation is recommended as a standard for reference evapotranspiration to provide values more consistent with actual global crop water use data (Allen et al., 2006). The PM equation is appropriate for assessing the present evapotranspiration (2004-2011), but not the future (2046-2065). The outputs of GCMs are precipitation and temperature, which are insufficient for calculating evapotranspiration through the PM equation. To overcome this problem, the Hamon method (Shaw and Riha, 2011), a temperature-based equation, was adopted. Linear regression was also applied to adjust the bias between the PM equation and the Hamon method.

2) Parameter Calibration

A total of eight parameters of the two-layer tank model were calibrated (Fig. 3) by using genetic algorithm (GA). GA is an effective and powerful tool for solving optimization problems (Holland, 1975). As an evolution algorithm, the GA is based on the concept developed Darwin, "living things compete, nature selects, the fittest survive". In GA, a set of parameters is compared to a chromosome. The first step involves generating chromosomes randomly and estimating the fitness. The next step is selection. In general, the higher the fitness is, the greater the chance is that the chromosome is selected. After two chromosomes are selected, a crossover mechanism generates new chromosomes as offspring, according to the parents. The core function of the crossover is to explore improvement possibilities in the given searching field. Mutation is an effective mechanism for preventing the optimal solution from falling to a local minimum. The mutation probability should not be too high, or a divergent result occurs. Reproduction is a step that saves the fitter chromosomes that will form the initial population of the next generation. Finally, the optimal solution is obtained by repeating the steps from in subsequent generations (Fig. 4).

Table 1. Parameter Calibration according to the Genetic Algorithm.

Parameters	Setting
Number of variables	8
Coding	Real number
Initial population	200
Selection	Roulette
Crossover method and rate	All points arithmetic crossover 90%
Mutation method and rate	Uniform one point mutation 1%
Reproduction	Keep-best
Stop criterion	Runs 10,000 generations

Table 2. Searching ranges of tank model parameters.

Parameters	a0	a1	a2	ha1	ha2	b0	b1	hb1
Upper / lower limits	0-0.5	0-0.5	0-1	0-100	0-100	0-0.5	0-0.5	0-100
Unit	1/day	1/day	1/day	mm	mm	1/day	1/day	mm

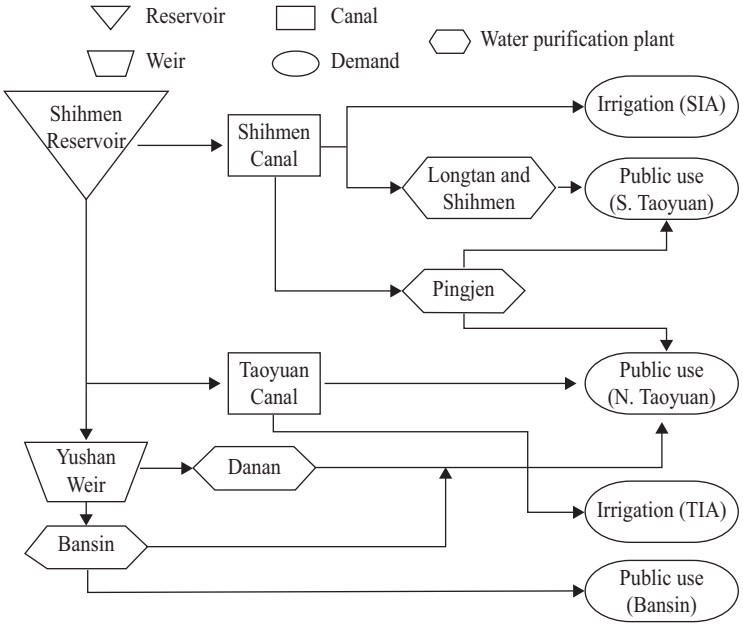

Fig. 5. Conceptual water supply system of the Shihmen reservoir.

The settings of a GA are listed in Table 1. Real number coding was adopted here because it is more accurate, more convenient and faster than traditional binary coding in many situations (Goldberg, 1991; Man et al., 2001). Roulette is a well-known method of selection; the chance that a chromosome has been selected for crossover depends on the proportion of its fitness relative to the summation of fitness. For the crossover mechanism, we chose all points of arithmetic crossover (Michalewicz, 1996), and set the crossover rate at 90%. Uniform one-point mutation is a common method for performing GA, and a mutation rate of 1% was used in this study. The method adopted for reproduction was keep-best reproduction (Wise and Goodwin, 1998). After the GA ran 10,000 generations, it was regarded as reaching the stop criterion and convergence. Table 2 shows the searching constraints of the tank model parameters for the GA.

The fitness function can be expressed as the following equation:

$$Fitness = \frac{\sum_{t=1}^{N} \frac{\left|O_{sim}(t) - O_{obs}(t)\right|}{O_{obs}(t)}}{N} \quad (1)$$

Here Q_{sim} and Q_{obs} are the simulated and observed inflow of the Shihmen reservoir; N is the number of days of calibration.

3) Water Supply System of the Shihmen Reservoir

A reservoir system simulation model reproduces the hy-

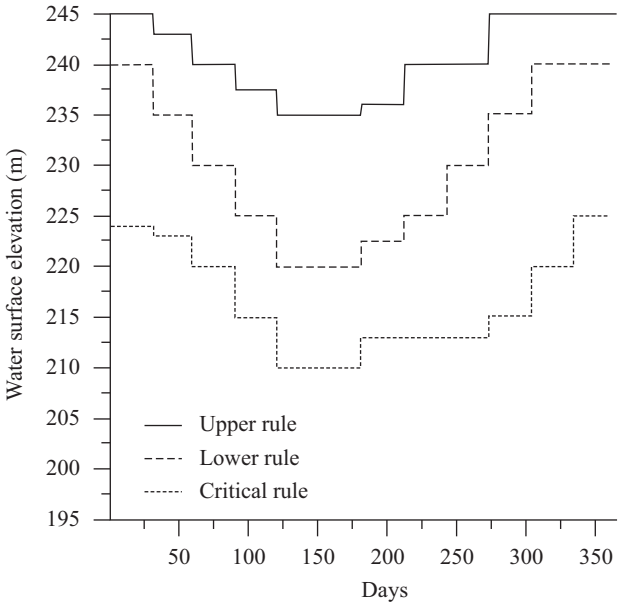

Fig. 6. Operation rule curves of the Shihmen reservoir.

drologic performance of a reservoir system for given inflows and operating rules. The models are based on mass-balance accounting procedures for tracking the movement of water through a reservoir-stream system (Wurbs, 1993). Fig. 5 represents the conceptual water supply system of the Shihmen reservoir. The definitions of upper, lower and critical rule curves are shown in Fig. 6. The Shihmen reservoir must supply public water to northern Taoyuan, southern Taoyuan, and the Banqiao-Xindian area (parts of New Taipei City, known as the Bansin area), and irrigation water to the SIA and the TIA areas. According to "The Operational Regulations of Shihmen Reservoir" (Water Resources Agency, 2013), the operation of the reservoir should follow these principles:

(1) Supply of the Shihmen reservoir must not be less than the projected demand if the water surface elevation exceeds the upper limit.
(2) Supply of the Shihmen reservoir should satisfy the projected demand if the water surface elevation is between the upper and lower limit.
(3) Supply of the Shihmen reservoir should satisfy 75% of the projected irrigation demand and 90% of the projected public demand if the water surface elevation is between the lower and critical limit.
(4) Supply of the Shihmen reservoir should satisfy 50% of the projected irrigation demand and 80% of the planning public demand if the water surface elevation is under the critical limit.

If the volume of the reservoir is too low to meet the demand mentioned in principle (4), the government would consider a stricter strategy for water saving, for example, farmland fallow.

Unlike the second cropping season (August-November), the first cropping season (March-June) for the SIA and the TIA usually coincides with drought because it occurs after the dry season (October-April) of the Shihmen watershed. Therefore, the mechanism of irrigation fallow should be considered for the first cropping season. In practice, decision makers choose which area to fallow in the following year according to the projected severity of the drought. However, it is difficult to formulate the relation between the severity of drought and areas of fallow, in part because of uncertainty regarding the attitudes of the decision makers. We made the fallow mechanism simple and logical, so that it could be programmed. Therefore, we assumed that in extreme droughts, such as when the reservoir is empty, at least one of the irrigation associations would fallow the entire area. Although the theoretical fallow mechanism does not match the current practice, we believe that it is an effective and approximate model to follow.

The following are the irrigation fallow mechanisms in our simulation:

(1) The program resets the demand of the TIA to 0 if the reservoir storage becomes empty during the first cropping season and restarts the simulation from the first day of the year.
(2) The program will reset the demands of the SIA and the TIA to 0 if the reservoir storage becomes empty during the first cropping season after step 1 has been completed and restarts the simulation from the first day of the year.

Once the reservoir becomes empty during the first cropping season, the whole area of the TIA is fallowed. If the reservoir remains empty, the TIA and SIA irrigation areas are fallowed simultaneously.

4) Demand

Huang et al. (2013) and Lee and Huang (2014) have discussed the future irrigation water requirements of both the SIA and the TIA. The rainfall and temperature projections for 2046-2065 were adopted from five downscaled GCMs. The future evapotranspiration was derived from the Hamon method and corrected with the quadrant transformation method. On the basis of the projections and the water balance model in paddy fields, future crop water requirements, effective rainfall and irrigation demand could be calculated (Lee and Huang, 2014). Fig. 7 shows the present (2004-2011) and future (2046-2065) irrigation water requirements. Notice that the average requirement in the future is the ensemble mean of the results of the five GCMs and not the result of the mean temperature and rainfall of these GCMs. The projected summation of irrigation requirements in the future is approximately $0.5\text{-}2.0 \times 10^6$ m^3/ten-days.

The daily demands of northern Taoyuan, southern Taoyuan, and the Bansin area are 5.7, 6.8 and 5.0×10^5 m^3/day, respectively. We assumed they were the basic loadings for public use and that they remained constant in the present and future. The development of the Taoyuan Aerotropolis is an impending source of water supply pressure on the Shihmen reservoir. The first part

Table 3. The optimal parameters of the Tank model.

Parameters	a0	a1	a2	ha1	ha2	b0	b1	hb1
Value	0.11167	0.11232	0.29017	24.57	97.80	0.01046	0.03759	17.17
Unit	1/day	1/day	1/day	mm	mm	1/day	1/day	mm

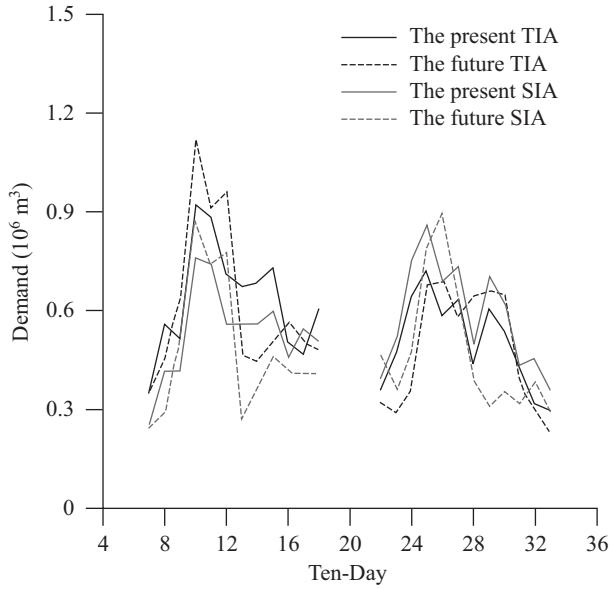

Fig. 7. Average irrigation water requirements of SIA and TIA in the cropping seasons.

of this project will increase demand by approximately 7.3 × 10^4 m^3/day.

Consequently, the projected demand of future cropping seasons is approximately 1.8-2.0 × 10^6 m^3/day. If the demand of the Taoyuan Aerotropolis is considered, the projected demand is approximately 1.9-2.0 × 10^6 m^3/day.

5) Indices for Iimpact and Risk Assessment

To assess the impact and the risk under climate change and development scenarios, the shortage index (SI), satisfaction and reliability of the water supply were determined. Eqs. (2)-(4) define these indices.

$$SI = \frac{100}{N}\sum_{t=1}^{N}\left(\frac{\left|Q_d - Q_{\sup}\right|}{Q_d}\right)^2 \quad (2)$$

$$Satisfaction = \frac{Q_{\sup}}{Q_d}\times 100\% \quad (3)$$

$$Reliability = \frac{N_{sat}}{N}\times 100\% \quad (4)$$

Here Q_d and Q_{sup} are the quantities of water demand and supply, respectively; N is the given time scale of the simulation, and N_{sat} is the number of days for which the demand has been satisfied.

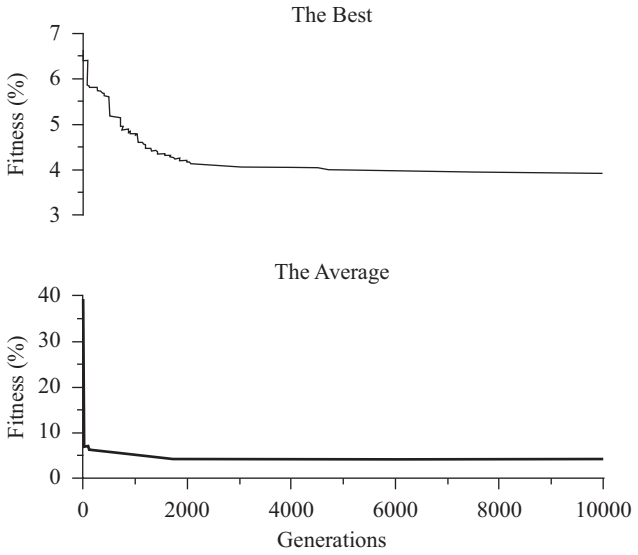

Fig. 8. The best and average fitness of generations.

3. Results and Discussion

1) Tank Model Validation

The optimal parameters and the efficacy of the tank model are discussed. The two-layer tank model had eight parameters that required calibration. According to the constraints and fitness functions mentioned in section 2.2, the GA assisted in obtaining the optimal solution. However, some parameters that were necessary for the PM equation were unavailable for 2004-2007; therefore, we were limited to the 2008-2012 data. We calibrated the parameters of the tank model with the 2008-2010 data, and used the two remaining years (2011-2012) for validation purposes.

Fig. 8 illustrates the variation in the fitness values used for calibration. After 10,000 generations, the fitness values become convergent. Moreover, the average fitness of the final generation is 4.06, whereas the fitness of the optimal solution is 3.93. The optimal parameters are listed in Table 3, and they have physical meaning. For example, anisotropic aquifers are common in nature and cause different velocities of hydraulic conductivity between horizontal and vertical directions. The velocity of horizontal hydraulic conductivity is generally higher than that of vertical hydraulic conductivity. These phenomena were observed in the tank model parameters: the bottom orifices (a0 and b0) are smaller than the others (a1, a2 and b1) for each layer. Moreover, the depth of the surface increases during rainstorms, the watershed outflow increases significantly and nonlinearly, explaining why orifice a2 is larger than orifice a1.

Fig. 9 illustrates that the two-layer tank model can simulate the inflow time series and capture the seasonal variation of the Shihmen watershed. Table 4 shows the result of the error between the simulation and the observation. The annual dif-

Table 4. The error of validation of 2011-2012 between the simulated and the observed discharge.

Discharge (m^3/s)	Observed	Simulated	Error (%)	RMSE (m^3/s)
Annual	38,399.95	33,776.95	-12.04	97.96
Dry season	9,848.20	8,543.04	-13.25	49.17
Wet season	28,551.75	25,233.87	-11.62	156.81

Table 5. Projected rainfall and inflow over the Shihmen reservoir basin.

Daily discharge (m^3/s)		Present	CCCma	CNRM	CSIRO	GFDL	LASG
Precipitation (mm)	**Annual**	2709.68	2624.74	2176.98	2411.86	2734.72	2663.24
	Dry season	704.52	792.48	564.00	563.97	846.43	830.04
	Wet season	2005.16	1832.26	1612.99	1847.89	1888.29	1833.20
Inflow	**Annual**	48.37	42.31	33.19	37.61	42.86	41.91
	Dry season	23.41	25.53	17.12	17.97	27.10	26.80
	Wet season	72.92	58.82	49.01	56.92	58.35	56.78

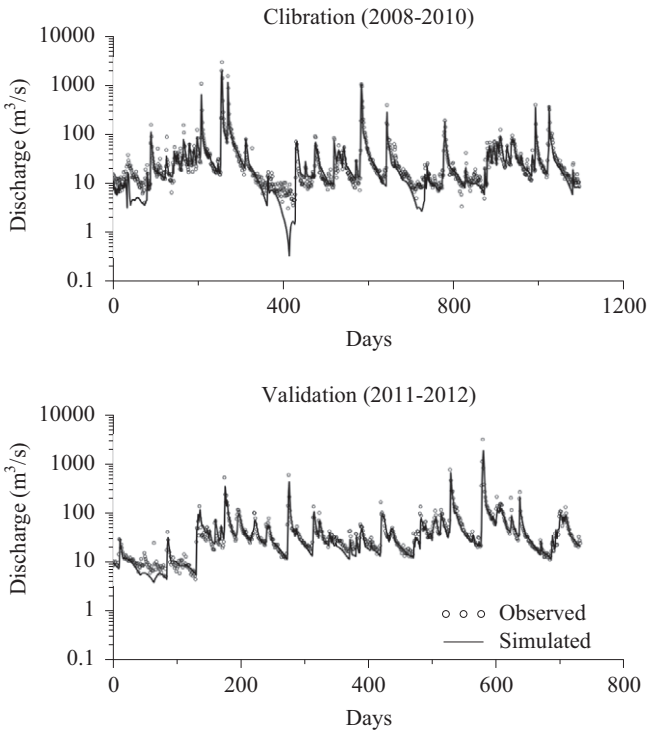

Fig. 9. The comparison between observed and simulated discharge time series.

ference of total inflow is -12.04%, and the root mean square error (RMSE) is 97.96 m^3/s. In the dry season (November-April), the difference and the RMSE between the simulation and observation are -13.25% and 49.17 m^3/s, respectively. In the wet season (May-October), the difference and the RMSE are -11.62% and 156.81 m^3/s, respectively. Although the relative error of the dry season is the highest, its RMSE is the lowest. This is because the comparison foundations of the different periods were not the same. On this basis, we preferred to make judgments by using the RMSE. The RMSE indicated that the simulation result of the dry season is more favorable than that of the wet season. Accurately simulating floods is not the focus of the water supply operation of a reservoir. Thus, the relative error is acceptable and the tank model was adopted.

2) Impact of Climate Change on Reservoir Inflow

The reservoir inflow of the present (1993-2012) and future (2046-2065) are displayed in Table 5. All annual inflow values are significantly lower in the projections than in the present. In the dry season, the difference between the present and the GCMs outputs is nonsignificant. By contrast, a significant decrease in inflow was observed in the wet season regardless of the average temperature or precipitation. The decrement of inflow results from the decrease in projected precipitation. In fact, the inflow values during typhoons were difficult to estimate through the tank model, which may have led to an underestimation.

3) Impact of Climate Change on the Water Supply

We considered farming with and without irrigation fallow, and the development of the Taoyuan Aerotropolis; thus, four states are discussed. Fig. 10 displays the framework of the discussion.

State 1

State 1 involves farming without irrigation fallow and does not consider the Taoyuan Aerotropolis. The simulation results are shown in Table 6. For the present period, the public SI is 0.24 and the maximum consecutive dry days (MCDD) of public use is 69 days/yr. This indicate that drought is not presently a serious threat. However, all GCMs except the GFDL (only on

Table 6. Indices of the water supply for state 1.

Unit: quantity of water in 10^6 m^3/yr; MCDD in days/yr	Present	Ensemble in the future	CCCma	CNRM	CSIRO	GFDL	LASG
Public shortage	26.0	37.2	29.1	58.2	54.6	25.8	18.0
Shortage of SIA	12.5	17.0	12.9	26.6	22.3	15.7	7.5
Shortage of TIA	16.0	21.4	15.4	32.5	28.4	18.9	11.6
Reservoir supply	1,142.1	1,031.7	1,062.7	907.0	935.1	1,114.2	1,139.3
Reservoir overflow	488.2	147.9	201.8	76.9	184.7	165.9	110.4
Public SI	0.24	0.56	0.31	1.18	0.95	0.22	0.13
Public MCDD	69	93	73	132	136	72	50
MCDD of SIA	14	16	12	24	19	15	10
MCDD of TIA	13	17	12	22	23	16	12

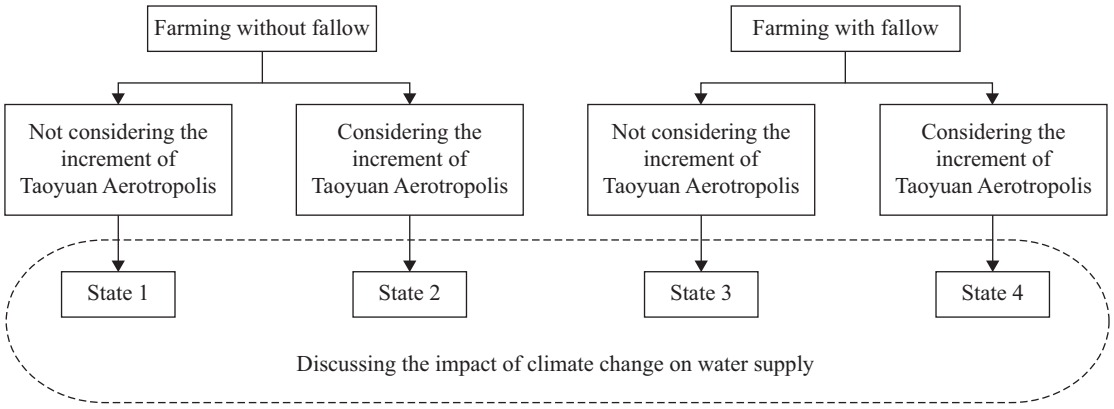

Fig. 10. Framework of possible alternatives.

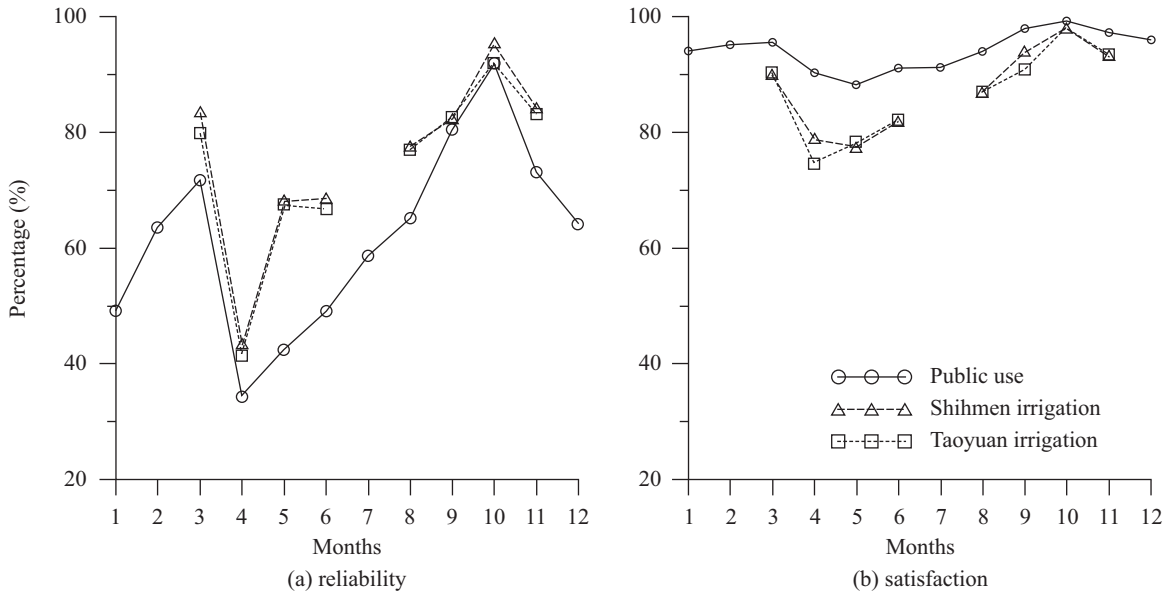

Fig. 11. The monthly reliability and satisfaction of the water supply in the future for state 1.

public water use) and LASG models, suggest worse conditions in the future. The drought of the ensemble projections is more severe because of lower reservoir supply.

According to Fig. 11, the monthly reliability is between 34.4% (in April) and 92.0% (in October); the monthly satisfaction is between 88.3% (in May) and 99.2% (in October).

Table 7. Indices of water supply for state 2.

Unit: quantity of water in 10^6 m^3/yr; MCDD in days/yr	Present	Ensemble in the future	CCCma	CNRM	CSIRO	GFDL	LASG
Public shortage	26.0	42.5	33.9	65.9	61.4	30.1	21.4
Shortage of SIA	12.5	18.4	14.1	28.4	23.7	17.2	8.4
Shortage of TIA	16.0	22.9	16.7	34.4	30.1	20.5	13.0
Reservoir supply	1,142.1	1,035.0	1,066.8	909.9	938.9	1,117.0	1,142.3
Reservoir overflow	488.2	145.2	198.5	75.0	181.9	163.3	107.5
Public SI	0.24	0.65	0.37	1.36	1.09	0.28	0.17
Public MCDD	69	99	81	135	148	77	56
MCDD of SIA	14	16	12	25	19	16	10
MCDD of TIA	13	18	13	22	23	17	13

Table 8. Indices of the water supply for state 3.

Unit: quantity of water in 10^6 m^3/yr; MCDD in days/yr	Present	Ensemble in the future	CCCma	CNRM	CSIRO	GFDL	LASG
Public shortage	22.4	27.3	23.3	36.3	39.6	21.0	16.2
Shortage of SIA	10.2	10.6	10.6	11.5	12.1	12.3	6.5
Shortage of TIA	8.9	10.4	11.2	9.1	11.5	10.5	9.9
Reservoir supply	1,138.8	1,028.5	1,060.7	899.6	931.1	1,112.6	1,138.4
Reservoir overflow	491.3	149.5	202.4	80.6	186.9	166.6	111.0
Public SI	0.16	0.26	0.18	0.39	0.49	0.14	0.10
Public MCDD	58	76	67	93	101	69	48
MCDD of SIA	12	13	12	17	14	13	9
MCDD of TIA	7	12	11	13	14	13	10
Annual fallow times of SIA	0	3	1	7	6	1	1
Annual fallow times of TIA	2	7	4	13	11	6	1

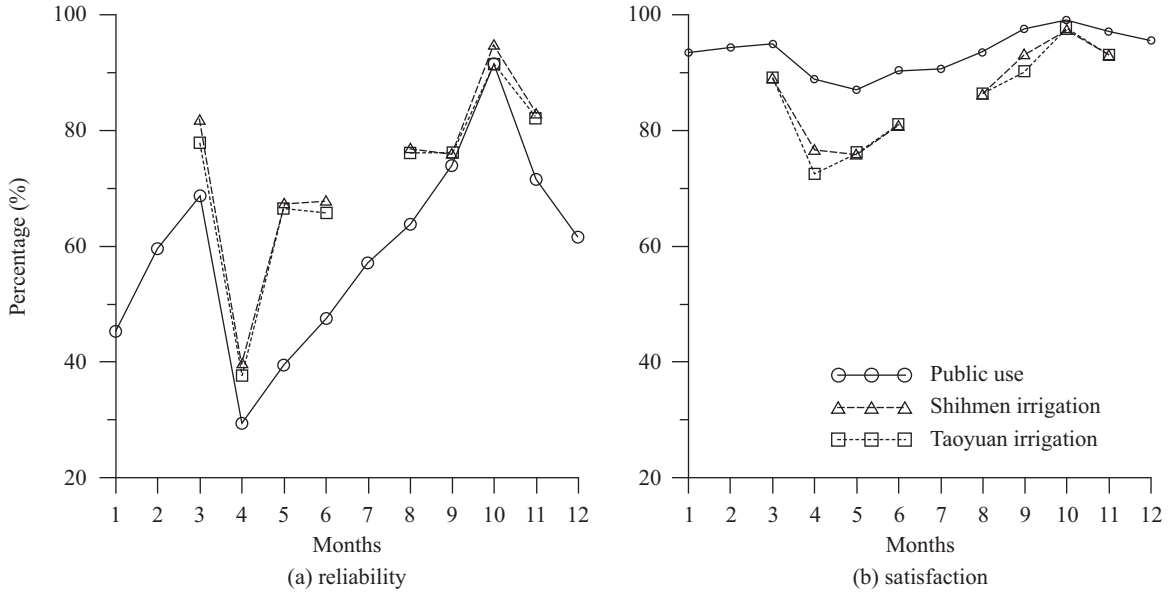

Fig. 12. The monthly reliability and satisfaction of the water supply in the future for state 2.

State 2

State 2 considers farming without irrigation fallow but with the development of the Taoyuan Aerotropolis. Table 7 displays the simulation results. In the present period, the results identical to those of in state 1. In the future, except for the LASG model, all GCMs indicate worse conditions than the present conditions. The water shortage of the ensemble in the future is more severe as well.

As displayed in Fig. 12, the monthly reliability is between

Table 9. Indices of the water supply for state 4.

Unit: quantity of water in 10^6 m^3/yr; MCDD in days/yr	Present	Ensemble in the future	CCCma	CNRM	CSIRO	GFDL	LASG
Public shortage	22.4	31.2	27.0	42.3	43.5	24.0	18.9
Shortage of SIA	10.2	10.9	11.2	11.8	11.3	13.0	6.9
Shortage of TIA	8.9	10.1	10.9	10.5	9.1	10.2	10.0
Reservoir supply	1,138.8	1,032.0	1,064.2	903.1	935.6	1,115.3	1,141.6
Reservoir overflow	491.3	146.4	199.4	77.7	183.0	163.9	107.9
Public SI	0.16	0.31	0.22	0.49	0.53	0.18	0.12
Public MCDD	58	81	75	95	109	74	53
MCDD of SIA	12	13	12	16	14	13	9
MCDD of TIA	7	12	11	15	12	13	9
Annual fallow times of SIA	0	4	1	9	7	1	1
Annual fallow times of TIA	2	8	5	13	13	7	2

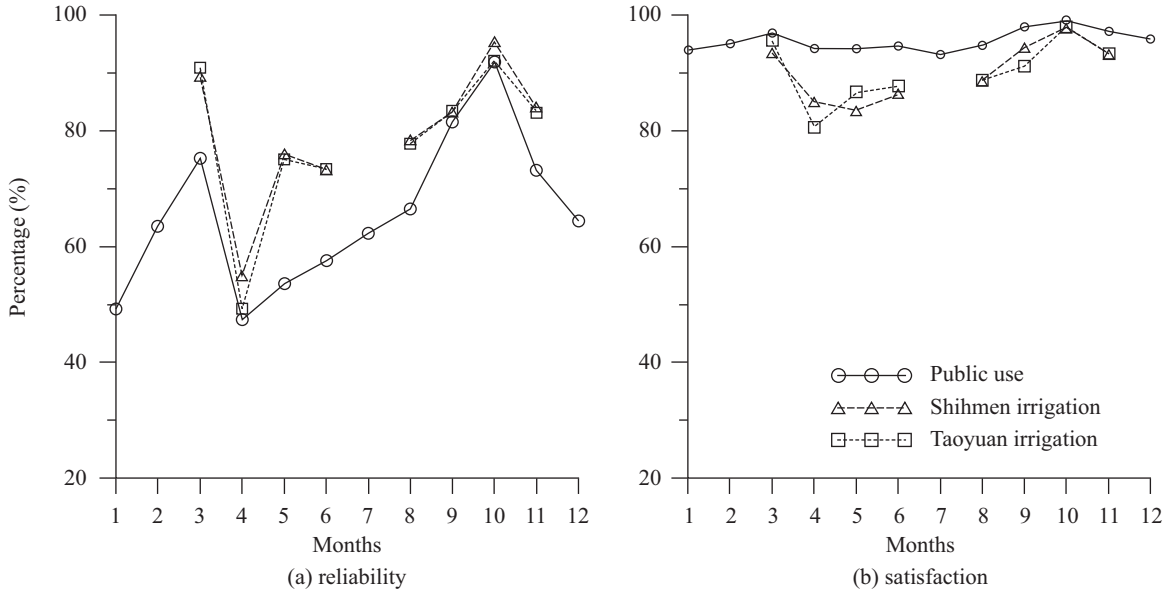

Fig. 13. The monthly reliability and satisfaction of the water supply in the future for state 3.

29.4% (in April) and 91.4% (in October); the monthly satisfaction is between 87.1% (in May) and 99.1% (in October).

State 3

State 3 includes irrigation fallow but does not consider the Taoyuan Aerotropolis. The simulation results are shown in Table 8. For the present period, the public SI is 0.16 and the MCDD of public use is 58 days/yr. Irrigation fallow for the TAI occurs two times annually on average, but no irrigation fallow occurs for the SIA. The results of all the GCMs, except the GFDL (only on public water use) and LASG models, indicate worse conditions than the present conditions. The decreasing reservoir supply results in a more severe drought.

As demonstrated in Fig. 13, the monthly reliability is between 47.5% (in April) and 92.1% (in October); the monthly satisfaction is between 93.3% (in July) and 99.2% (in October).

State 4

State 4 includes farming with irrigation fallow and considers the development of the Taoyuan Aerotropolis. Table 9 displays the simulation results. For the present, the results are the same as those of in state 3. In the future, except for the LASG model, all the GCMs predict worse conditions than those of the present. The water shortage of the ensemble is more severe in the future as well.

As outlined in Fig. 14, the monthly reliability is between 43.3% (in April) and 91.5% (in October); the monthly satisfaction is between 92.9% (in July) and 99.2% (in October).

4. Concluding Remarks

As described in section 3-1, the parameters of the tank model used to simulate the inflow of the Shihmen watershed were ca-

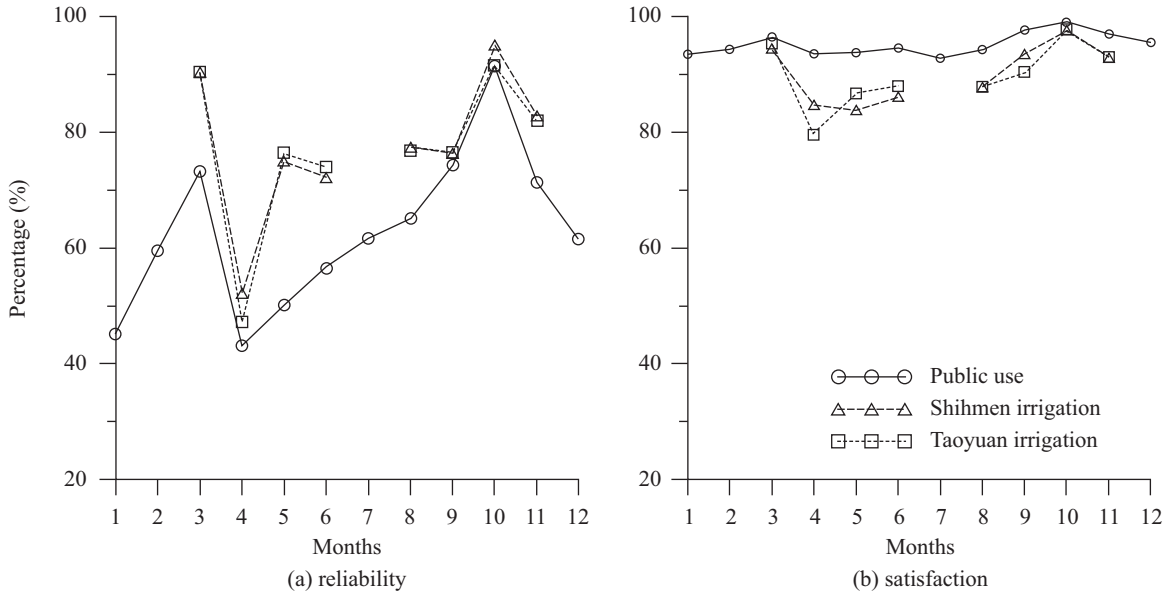

Fig. 14. The monthly reliability and satisfaction of the water supply in the future for state 4.

librated and validated. The results indicate that inflow will decrease in the wet season (May-October) in the future (2046-2065), which will be the main reason for the decrease in annual precipitation (Table 5).

Because of decreasing reservoir inflow, most of the simulation results of the GCM projections reveal that the water shortage will increase in severity. Although the public SI of state 1 and 2 in the future are approximately 0.6 (Tables 6 and 7, respectively), which would be suitable, it is over two times that of the public SI in the present period (0.24). The monthly water supply (Figs. 11 and 12) suggests that drought is most severe during the first cropping season of the year. Thus, the water supply risk is high from March to June in the future.

For the states including irrigation fallow (states 3 and 4), the public SI is reduced to approximately 0.3 (Tables 8 and 9) in the future, less than two times that of the present (0.16). Meanwhile, the monthly reliability and satisfaction of the water supply are improved significantly (Figs. 13 and 14). If satisfying the demand of public use is the top priority, irrigation fallow during the first cropping season is required to combat the effects of climate change.

ACKNOWLEDGEMENTS

The authors express appreciation to the National Taiwan University Global Change Center for providing relevant downscaled GCMs. This study was sponsored by a project of the Council of Agriculture under the Executive Yuan of Taiwan (102AS-8.2.4-IE-b2 and 103AS-8.2.6-IE-b1).

REFERENCES

Allen, R. G., L. S. Pereira, D. Raes and M. Smith (2006). FAO irrigation and drainage paper NO. 56 - crop evapotranspiration. Food and Agriculture Organization of the United Nations.

Asia Development Bank (2009). Climate Change and Migration in Asia and the Pacific. In: Identifying Hot Spots of Climate Change Impact, edited by The University of Adelaide, Flinders University and The University of Waikato. Asia Development Bank, Mandaluyong City, Philippines, 15.

Goldberg, D. E. (1991). Real-coded Genetic Algorithms, Virtual Alphabets, and Blocking. Complex Systems 5, 139-167.

Hsu, H. H., C. Chou, Y. C. Wu, M. M. Lu, C. T. Chen and Y. M. Chen (2011). Climate Change in Taiwan: Scientific Report 2011 (Summary). National Science Council, Executive Yuan, Taiwan.

Huang, W. C., Y. Chiang, R. Y. Wu, J. L. Lee and S. H. Lin (2012). The impact of climate change on rainfall frequency in Taiwan. Terrestrial. Atmospheric and Oceanic Sciences 23, 553-564.

Huang, W. C., Y. H. Wu and J. L. Lee (2014). Impact of climate change on rainfall in Taiwan during 2046-2065. Journal of Taiwan Agricultural Engineering 60, 1, 66-80. (in Chinese)

Huang, W. C., H. H. Yang and J. L. Lee (2013). Impact of climate change on irrigation water requirement for Shihmen irrigation area. Journal of Taiwan Water Conservancy 61(3), 87-97. (in Chinese)

IPCC (2007). Climate Change 2007: Synthesis Report. Contribution of Working Groups I, II and III to the Fourth Assessment Report of the Intergovernmental Panel on Climate Change, edited by Core Writing Team, Pachauri, R. K. and Reisinger, A. IPCC, Geneva, Switzerland.

IPCC (2014). Climate Change 2014: Synthesis Report, Summary for Policymakers. Contribution of Working Groups I, II and III to the Fifth Assessment Report of the Intergovernmental Panel on Climate Change, edited by Core Writing Team, Pachauri, R.K. and Meyer, L.A. IPCC, Geneva, Switzerland.

Holland, J. H. (1975). Adaptation in Natural and Artificial Systems. University of Michigan Press, Michigan, U.S.A.

Kalnay, E., M. Kanamitsu, R. Kistler, W. Collins, D. Deaven, L. Gandin, M. Iredell, S. Saha, G. White, J. Woollen, Y. Zhu, M. Chelliah, W. Ebisuzaki, W. Higgins, J. Janowiak, K. C. Mo, C. Ropelewski, J. Wang, A. Leetmaa, R. Reynolds, R. Jenne and D. Joseph (1996). The NCEP/NCAR 40-year reanalysis project. Bulletin of the American Meteorological Society 77, 437-470.

Lee, J. L. and W. C. Huang (2014). Impact of climate change on the irrigation water requirement in Northern Taiwan. Water 6, 3339-3361.

Lin, S. H., Y. C. Chen, W. S. Lin and C. M. Liu (2009). Climate change projection for Taiwan based on statistical downscaling on daily temperature and precipitation. The 15th International Joint Seminar on the Regional Deposition Processes in the Atmosphere and Climate Change, Taipei, Taiwan.

Lin, S. H., C. M. Liu, W. C. Huang, S. S. Lin, T. H. Yen, H. R. Wang, J. T. Kou and Y. C. Lee (2010). Developing a yearly warning index to assess the climatic impact on the water resources of Taiwan, a complex-terrain island. Journal of Hydrology 309, 13-22.

Liu, C. M., S. H. Lin, S. H. Schneider, T. L. Root, K. T. Lee, H. J. Lu, P. F. Lee, C. Y. Ko, C. R. Chiou, H. J. Lin, C. F. Dai, K. T. Shao, W. C. Huang, H. S. Lur, Y. Shen and C. C. King (2008). Climate change impact assessment in Taiwan. Global Change Research Center National Taiwan University, Taipei, Taiwan.

Man, K. F., K. S. Tang and S. Kwong (2001). Genetic Algorithms: Concepts and Designs, third edition. Chapter 2, 24. Springer-Verlag London, London, U.K.

Michalewicz, Z. (1996). Genetic Algorithms + Data Structures = Evolution Programs, third edition. Springer-Verlag Berlin Heidelberg, New York, U.S.A.

Northern Region Water Resources Office (2014). The website for a introduction of the Shihmen Reservoir: http://www.wranb.gov.tw/ct.asp?xItem=1199&ctNode=323&mp=5, Water Resources Agency, Ministry of Economic Affairs, Taiwan.

Shaw, S. B. and S. J. Riha (2011). Assessing temperature-based PET equations under a changing climate in temperate, deciduous forests. Hydrological Processes 25, 1466-1478.

Sugawara, M. (1985). Lecture Note of Hydrologic Modeling by Tank Model. Department of Civil Engineering, National Taiwan University, Taipei, Taiwan.

Water Resources Agency (2013). The Operational Regulations of Shihmen Reservoir. Water Resources Agency, Ministry of Economic Affairs, Taiwan. (in Chinese)

Wise, K. and S. D. Goodwin (1998). Keep-best reproduction: A selection strategy for genetic algorithms. Proceedings of the 1998 ACM Symposium on Applied Computing, 343-348.

Wurbs, R. A. (1993). Reservoir-System Simulation and Optimization Models. Journal of Water Resources Planning and Management 119(4), 455-472.

Wu, Y. C., H. H. Hsu, C. Chou, M. M. Lu, C. T. Chen and Y. M. Chen (2013). An introduction to climate change in Taiwan: Scientific report 2011. APEC Research Center for Typhoon and Society Newsletter 3, 1, 16-19.

Yokoo, Y. and S. Kazama (2012). Numerical investigations on the relationships between watershed characteristics and water balance model parameters: Searching for universal relationships among regional relationships. Hydrological Processes 26, 843-854.

Yu, P. S. (2006). Trend and variability analysis of drought in Taiwan (I). National Science Council, Executive Yuan, Taiwan. (in Chinese)